Chinese Journal of Chemical Engineering 87 (2025) 357–368

Contents lists available at ScienceDirect

Chinese Journal of Chemical Engineering

journal homepage: www.elsevier.com/locate/CJChE

Full Length Article

Decoupling combustion of coal briquettes and coal-biomass blends in a pilot-scale test facility for novel grate boilers

Xinhua Liu [1,2,*], Bin Liang [1,2], Jian Han [1,2], Shanwei Hu [1,2,*]

[1] State Key Laboratory of Mesoscience and Engineering, Institute of Process Engineering, Chinese Academy of Sciences, Beijing 100190, China
[2] School of Chemical Engineering, University of Chinese Academy of Sciences, Beijing 100049, China

A R T I C L E I N F O

Article history:
Received 20 December 2024
Received in revised form
10 April 2025
Accepted 6 May 2025
Available online 6 August 2025

Keywords:
Decoupling combustion
NO_x emission
Coal briquette
Straw pellet
Medicine residue
Grate boiler

A B S T R A C T

With the increasingly stringent national environmental protection policies, the ultra-low emission transformation of industrial coal-fired grate boilers and the highly efficient utilization of biomass resources or wastes are becoming increasingly urgent in China. This study first proposes a novel and simple configuration for industrial grate boilers to integrate the decoupling combustion and flue gas recirculation or co-firing technologies, so as to reduce pollutant emission but improve thermal efficiency. Burning coal briquettes in the novel grate boiler, the original NO_x emissions can be remarkably decreased to as low as 56 $mg\cdot m^{-3}$, corresponding to the reduction efficiency of 82.8% in comparison with the average value in traditional coal-fired grate boilers. Co-firing coal briquettes with straw pellets in the novel grate boiler, the strongest synergistic effect of NO_x reduction is observed at the blending mass fraction of 50%, in which the NO_x emissions can be further mitigated by at most 16.0% on top of the already reduced amount by decoupling combustion to reach less than about 165 $mg\cdot m^{-3}$. The novel grate boiler allows co-firing Chinese medicine residue with high water content at the blending mass fraction of up to 30% on the premise of low NO_x and CO emissions. All experimental results in this study demonstrated the obvious superiorities of the novel grate boiler in reducing NO_x and CO emissions and mitigating both slagging tendency and slag carbon content, which can be attributed to either the cumulative effects of decoupling combustion with flue gas recirculation or the synergistic effects of co-firing coal-biomass blends. The newly-developed travelling-grate decoupling combustion technology can be expected to provide an economical and convenient measure for the ultra-low NO_x emission transformation of industrial coal-fired grate boilers as well as the clean and highly efficient consumption of biomass wastes with high water content or difficulty to burn in China.

1. Introduction

Coal is taken as one of the primary boiler fuels in China to provide heat, hot water, steam, or electricity due to its wide availability, low cost, and high calorific value although large amounts of air pollutant emissions arise from coal combustion in domestic and industrial boilers [1]. With the proposal of carbon peaking and carbon neutrality goals, biomass is also highly recommended for residential and industrial uses in China because of its renewability and carbon neutralization [2]. Through co-firing biomass and coal, lower combustion characteristic temperature and higher volatile content of biomass have been proven to result in the improvement of coal combustion performance as well as the reduction of NO_x emissions of 10% to 27% [3–5]. In addition, the slagging and fouling tendency of blending fuels was also alleviated in comparison with biomass itself [6]. Owing to the complementarity between the fuel properties and combustion characteristics of coal and biomass, co-firing coal and biomass has been thought to be a promising way to achieve the efficient and clean combustion of blending fuels in circulating fluidized bed boilers for power generation, which was however seldom applied in industrial grate boilers [7].

The average original emission concentration of NO_x in flue gas was reported to be about 325 $mg\cdot m^{-3}$ in bituminous coal-fired travelling grate boilers in China [8]. By modulating combustion intensity and reaction atmosphere, many denitrification

* Corresponding authors.
E-mail addresses: xhliu@ipe.ac.cn (X. Liu), swhu@ipe.ac.cn (S. Hu).

https://doi.org/10.1016/j.cjche.2025.05.040

technologies during combustion including flue gas recirculation (FGR), gas reburning, staged combustion, low-oxygen combustion and co-firing blends, *etc*., have been developed to mitigate NO_x emissions in industrial grate boilers, since the flue gas NO_x reduction technologies after combustion such as selective catalytic reduction (SCR) and selective non-catalytic reduction (SNCR) are generally expensive and complex. In these denitrification approaches during combustion, the FGR technology was characterized by the recirculation of less than about 25% of flue gas into the boiler, which lowered reaction temperature and oxygen content in the combustion region and resulted in NO_x emission reduction and boiler efficiency improvement by 10% to 30% and 2% to 3%, respectively [9,10]. However, the NO_x emissions are generally difficult to meet stringent standards with separate denitrification technology, thereby calling for the combinative application of different denitrification technologies. For instance, the denitrification efficiency of SNCR coupling the FGR denitrification technology was reported to be up to 56% in an industrial coal-fired grate boiler [11,12].

In order to suppress multiple pollutant emissions from burning coal or biomass, decoupling combustion as one of air/fuel staged combustion technologies in essence was originally implemented by separating the hearth into two zones to decouple the pyrolysis and combustion processes of solid fuels, thus facilitating the first low NO_x pyrolysis and combustion of solid fuels under the low temperature oxygen-deficient atmosphere in one zone, and then the later effective NO_x reduction by pyrolysis gas and char under the high temperature air atmosphere in the other zone [13]. The decoupling combustion technology reduced approximately 40% NO_x and 90% CO emissions in comparison with the traditional updraft combustion mode for domestic stoves [14–17]. The application of decoupling combustion method in small and medium-sized coal-fired reciprocating grate boilers (1.4 – 2.8 MW, thermal) was proven to enable the mitigation of NO_x emissions of about 33% [8,18]. Even partially implementing decoupling combustion in traditional large-sized coal-fired travelling grate boilers (7 –14 MW, thermal), the NO_x emissions could also be reduced by more than 25% by introducing a pre-burning device without any modification of boiler hearth configuration [8,19].

The decoupling combustion method can be combined with other advanced combustion technologies to further improve combustion efficiency and lower air pollutant emissions. For example, co-firing biomass and bituminous coal in household decoupling combustion furnaces indicated that coal char layer together with biomass pyrolysis gas could facilitate much lower NO_x emissions than burning either coal or biomass separately [20–22]. In addition, coal significantly alleviated the slagging and fouling tendency of biomass while biomass obviously improved the combustion reactivity of coal. The coal combustion in industrial grate boilers *via* combining decoupling combustion and gas reburning showed the NO_x emission reduction of about 30% to 60% in comparison with the traditional combustion without air staging and/or gas reburning [18,23]. However, the gas reburning approach calls for injecting other gas fuels as reductive agents into the reburning zone [18,24,25].

Despite probable cumulative effects of decoupling combustion with FGR and possible synergistic effects of co-firing technology, few researches focused on the integration of decoupling and FGR technologies or the decoupling co-combustion of coal and biomass in industrial travelling grate boilers. One of the reasons may lie in that the traditional hearth structure of a travelling grate boiler makes it difficult to implement the decoupling combustion principle completely, in which the forward extension of rear arch enables the formation of a high temperature oxygen-rich atmosphere there, so as to ignite the upper surface of fuel bed in the front section of chain grate by the radiant heat from the front and rear arches as well as flue gas. Therefore, we proposed a novel hearth structure for a decoupling combustion travelling grate boiler and set up a pilot-scale test facility of 700 kW (thermal) for the novel grate boiler [26]. This article further aims to delve deeper into the underlying denitrification mechanisms by burning bituminous coal briquettes under different air distribution in the test facility integrating the FGR technology. On this basis, the decoupling combustion characteristics of various coal-biomass blends are experimentally investigated by quantifying the reduction of NO_x and CO emissions as well as slag carbon content, in order to validate the feasibility and superiority of the decoupling and FGR or co-firing combinative technology for industrial grate boilers.

2. Experimental

2.1. Structure and principle of the novel grate boiler

The premise to implement decoupling combustion in large travelling grate boilers is steady supply of sufficient heat for the ignition and pyrolysis of fuel in the front section of chain grate. As indicated in Fig. 1(a), the traditional fuel feeder is replaced by a pre-burning device in the novel grate boiler, which utilizes an inclined reciprocating grate to realize the fuel feed from the top inlet to the bottom travelling grate with the aid of gravity. Its manufacturing cost generally accounts for 10% to 20% of the complete cost of the whole boiler. During the start-up of boiler, some firewood is first added to cover the inclined stationary reciprocating grate and then the fuel is added to fill the whole pre-burning device. After the firewood and part of fuel (marked in red color) are ignited successively from the reciprocating grate bottom, the fresh fuel is continuously added from the top inlet while the reciprocating grate is started to feed both the ignited and fresh fuel down to the travelling grate. In this case, the ignited fuel underlays the upper fresh fuel (marked in black color) on the travelling grate to provide the necessary heat for the pyrolysis process. When the novel grate boiler operates normally, the effective thermal load of the pre-burning device generally takes up 5% to 15% of the overall boiler thermal load, which can be controlled by adjusting the inlet air of the pre-burning device. Owing to the introduction of the pre-burning device, the front arch in the traditional boiler is not necessary again, and the rear arch can be moved to the end section of grate to make gas combustibles fully contact with the high temperature fuel bed and to improve their residence time in the high temperature hearth. Compared with the separation of the household furnace hearth into the two functional zones [13–17], this simple and novel configuration of grate boiler has the wonder of using different approaches to achieve equally satisfactory results. The novel grate boiler can be divided into several functional zones: a devolatilization zone in the pre-burning device on the left, a burnout zone on the right, as well as a pyrolysis and combustion zone between the pre-burning device and the partition wall. The air burnout zone can be further divided into a high temperature burnout zone above the rear arch and a low temperature burnout zone below the rear arch. Accordingly, it is possible to fully implement air-staged decoupling combustion in the novel boiler by adjusting air distribution mode.

As shown in Fig. 1(b), the fuel is first devolatilized at the low temperature of about 900 °C and the excess air ratio of $\alpha < 1$ in the pre-burning device, during which fuel N is converted into char N and volatile N, and the latter generally contains large amounts of light N-containing intermediate components such as NH_3 and HCN. Then, this part of char and the fresh fuel are pyrolyzed at about 1000 °C and $\alpha < 1$ in the middle zone continuously,

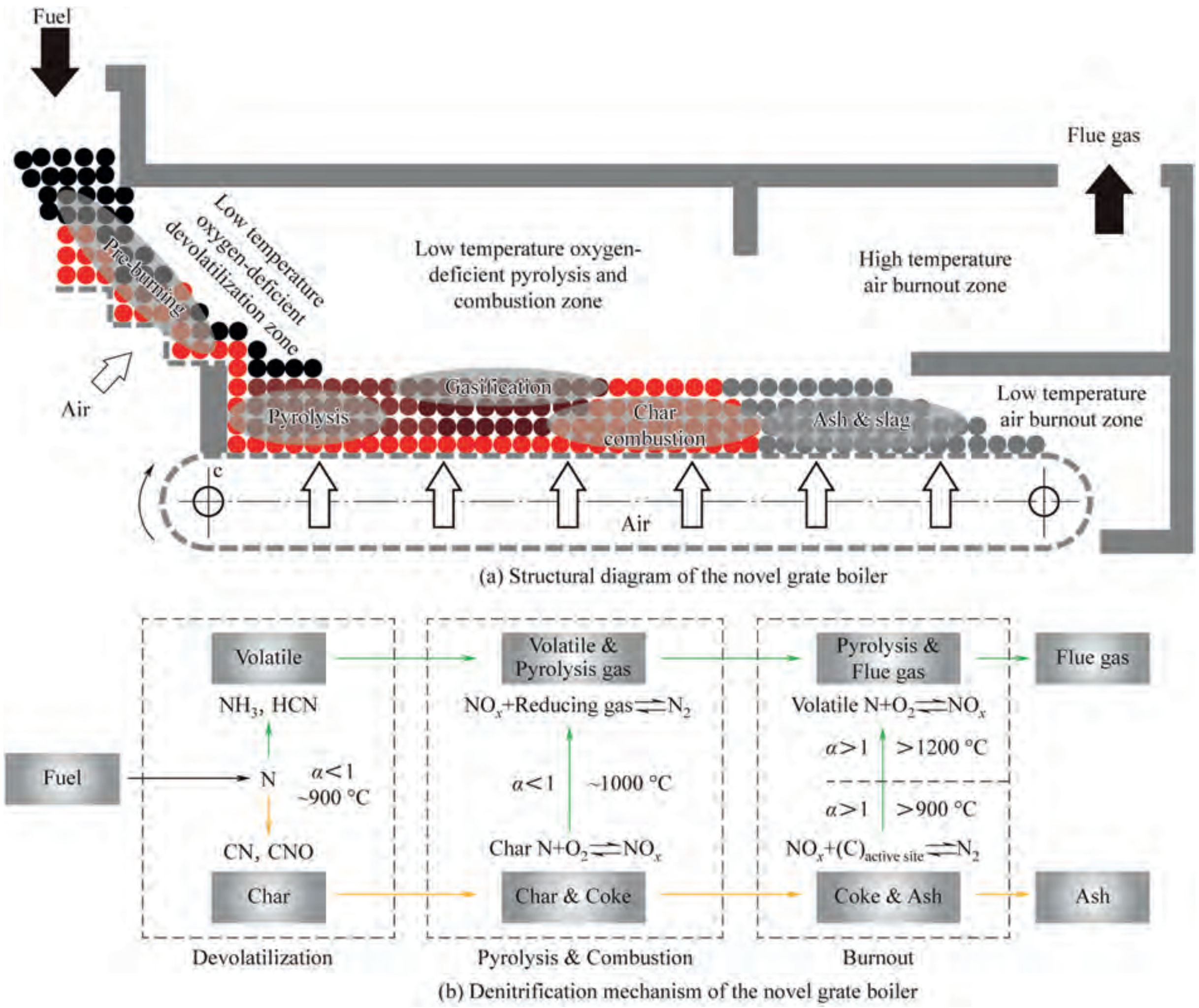

Fig. 1. Principle of travelling-grate decoupling combustion.

producing some reducing gas species including NH_3, HCN, CO and C_mH_n, *etc.* In this case, the conversion of volatile N to NO_x is significantly suppressed before the fuel on the grate approaches the position where the partition wall locates. On the other hand, even if part of char N is oxidized into NO_x in the middle zone, most of NO_x can also be reduced into N_2 by the aforementioned reducing gases during the nitrogen oxides are released from the fuel bed and mixed with the volatile and pyrolysis gases in the hearth [27]. Subsequently, the entire fuel bed from the bottom to the top begins to burn completely at the temperature higher than 900 °C and $\alpha > 1$ in the lower air burnout zone. Under this situation, a small amount of residual solid N in the resulted coke from char pyrolysis is oxidized into NO_x, part of which may however be converted to N_2 again by the high temperature char or coke layer itself because of its positive effect on NO_x reduction [15]. In the upper air burnout zone, if a part of volatile N is still not converted into N_2 completely, the residual may be oxidized into NO_x at the temperature higher than 1200 °C and $\alpha > 1$. Finally, this part of NO_x together with that resulted from the combustion of char N and coke N will be exhausted with flue gas. The ash and slag (marked in gray color) are also exhausted at the rear end of chain grate. Clearly, the lower NO_x emissions in the novel grate boiler than in the traditional grate boiler mainly depends on the homogeneous denitrification processes in the hearth with the oxygen-deficient atmosphere.

In the novel grate boiler, the fresh fuel is immediately ignited from bottom to top at the head of chain grate once it falls onto the burning fuel layer coming from the pre-burning device, which is equivalent to increasing the effective length of grate to improve its utilization efficiency. Besides this, the bottom-to-up ignition mode also contributes to the heterogeneous combustion of top fuel layer. These two factors lead to the significant increase of the burnout rate of large fuel particles, thus allowing the use of coal briquettes as fuel to decrease the leakage of granular coal or char but increase the thermal efficiency of grate boiler. Moreover, the introduction of pre-burning device enables the release of a part of volatile matter ahead of schedule and the extension of residence and combustion time of both gas combustibles and fuel particles in the hearth. As a result, the high temperature oxidizing atmosphere in the middle and rear hearth not only promotes the burnout of CO, but also provides grate potential for the NO_x emission reduction by combining the decoupling combustion and flue gas recirculation technologies, since a suitable amount of low temperature recirculated flue gas would not lead to remarkable decreases of temperature and oxygen content in both the hearth and the fuel bed [10,28].

2.2. Pilot-scale test facility and data acquirement

Fig. 2 shows the schematic diagram of piolet-scale decoupling combustion test facility for novel grate boilers. Inlet air supplied by an air blower was divided into six streams: one stream (pre-burning air) was supplied into the pre-burning device and the other five (primary air) into the main combustion chamber through five windboxes (i–v), whose horizontal distances from the pre-burning device are 1.15, 1.95, 2.7, 3.55 and 4.35 m, respectively. Each stream of airflow was adjusted by a valve and measured by a vortex flowmeter. Flue gas was cooled by three heat exchangers and then exhausted by an induced fan, part of which can be recirculated into either the middle freeboard of hearth or the windboxes under the chain grate by a recirculating fan.

An infrared gas analyzer (ABB AO2020, Germany) was used to online analyze original NO_x, CO and O_2 concentrations in outlet flue gas. Temperature profile in the hearth was measured by six thermocouples at the points of T1–T6, which were horizontally installed across the side wall to locate their measuring junctions at the middle of the boiler hearth. Their horizontal distances from the pre-burning device are 0.27, 1.07, 1.77, 2.47, 3.17 and 3.77 m, respectively. These experimental data were collected by a programmable logic controller and then recorded by a computer for successive analyses. All temperature and concentration data are time-averaged measuring values of at least 30 min when the test facility runs stably. Four gas sampling points a–d, whose horizontal distances from the pre-burning device are 0.15 m, 0.95 m, 2.55 m and 3.35 m, respectively, were set to measure gas species concentration profiles in the hearth by using a portable gas analyzer (Testo 340, Germany), in which the high-temperature-resistant sampling pipe of the portable analyzer was inserted into the middle of hearth across the side wall. The sampling measurement at each point was carried out at least 3 times at a 15-min interval, and the arithmetic mean of three independent measurements was taken as the final species concentration.

All NO_x and CO concentration values were corrected to the same dry oxygen basis of 9% (vol) for comparison,

$$C_{i,9\%O_2} = \frac{20.95 - 9.00}{20.95 - \phi_{O_2}} \times C_i \tag{1}$$

where C_i is the average mass concentration of gas component ($mg \cdot m^{-3}$); ϕ_{O_2} is the actual measured volumetric percentage of O_2 in flue gas (%, vol). In order to evaluate the combustion efficiency of solid fuels, the slag carbon contents under different operation cases were tested by using the ignition loss method according to GB/T34231—2017 in this study.

2.3. Tested bituminous coal and biomass fuels

A kind of ellipsoid bituminous coal briquettes with the size of 40 mm × 25 mm × 15 mm from three different batches (Coal a, Coal b and Coal c) was used as fuel or one of mixed components of blends in this study. Cylindrical straw pellets with the size of 8–10 mm in diameter and 30–60 mm in length as well as Chinese medicine residue with high water content were used as biomass fuels since they are typical representatives of agricultural biomass resources and high-water-content biomass wastes in China, respectively. Main properties of the tested coal and biomass fuels are shown in Table 1. It is clear that three batches of coal fuels have similar constituent properties. Straw pellets have much higher volatile and oxygen contents, but rather lower fixed carbon and ash contents than the coal fuels. Note that the water content of Chinese medicine residue as received basis is generally high up to about 50.0%, which causes difficulties in uniform micro sampling for property analysis and calorific value measurement. So, the proximate and ultimate analysis data of Chinese medicine residue as well as its net calorific value were measured on the air-dried basis, and then corrected to the values as received basis. It can also be found that the air-dried basis properties of Chinese medicine residue are similar to those of straw pellets as received basis.

2.4. Experimental cases for coal briquette combustion

Similar to decoupling combustion in household furnace [17], char bed depth and air distribution mode in the grate boiler are the most significant influence factors for the decoupling of pyrolysis and combustion processes, and thus affect pollutant emission and combustion efficiency. Using Coal a as the fuel, as shown in Table 2, five different operation cases (Cases I–V) were set to investigate the effects of fuel bed depth and air distribution mode. According to the calculated theoretical air volume needed for the running of test facility at the rated power, a total excess air coefficient of 1.3 was determined in all the cases in order to decrease boiler heat loss and ensure comparability among various operation cases. A

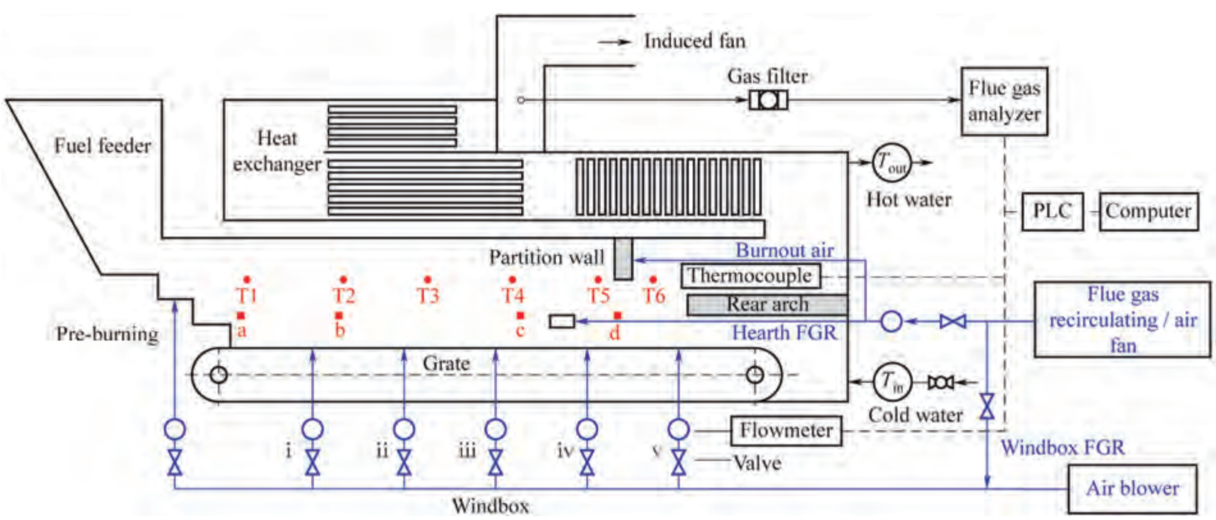

Fig. 2. Schematic diagram of the pilot-scale test facility for novel grate boilers.

Table 1
Properties of tested coal and biomass fuels.

Fuel	Proximate analysis (ar)/% (mass)				Ultimate analysis (ar)/% (mass)					$Q_{net,ar}$/MJ·kg^{-1}
	M	V	FC	A	C	H	O	N	S	
Coal a	7.0	26.7	47.0	19.3	56.7	3.9	12.1	0.80	0.20	21.9
Coal b	2.3	29.8	48.3	19.6	62.5	4.1	9.8	1.21	0.54	22.7
Coal c	7.3	25.9	43.1	23.7	54.5	4.2	8.7	0.80	0.29	19.8
Straw	9.2	75.6	6.4	8.8	42.5	3.9	31.0	4.40	0.19	14.3
Residue①	50.0	38.2	9.3	2.4	23.3	2.0	21.1	1.14	0.15	6.9

① Air dried basis data of residue: 3.1, 74.1, 18.1, 4.7; 45.1, 3.8, 40.8, 2.2, 0.30; 15.8.

uniform air distribution mode was adopted in Cases I–III while the fuel bed depth was determined as 120, 150 and 180 mm, respectively. An optimal fuel bed depth was set in Cases III–V, while the air distribution mode was set as the uniform, front-lean and rear-enhanced ones, respectively. In the uniform air distribution mode, the air flow ratios of five windboxes (i–v) are basically consistent, while the air flow ratios of windboxes i–ii and windboxes iv–v are relatively higher in the front-lean and rear-enhanced air distribution modes, respectively. In all the operation cases, the air flow ratio of the pre-burning device was fixed at about 20% in order to ensure the stable ignition and pyrolysis of a suitable amount of fuel.

This study also endeavors to examine the impact of flue gas recirculation (FGR) on nitrogen oxide emissions and coal combustion characteristics, so as to clarify the cumulative effects in the decoupling and FGR combinative combustion technology. Taking Case III adopting the optimal fuel bed depth and air distribution mode as a benchmark, the decoupling combustion with FGR was implemented by adopting hearth FGR and windbox FGR, respectively. As indicated in Fig. 2, in the hearth FGR the recirculated flue gas was directly introduced from a circulation port in the middle of hearth by a flue gas recirculating fan, while in the windbox FGR the recirculated flue gas was first mixed with primary air and then supplied into the windboxes. The hearth FGR ratio was set to vary from 5% to about 25%, while the windbox FGR ratio was adjusted to be less than about 15% since excessive windbox flue gas recirculation might result in a remarkable decrease of fuel bed temperature.

2.5. *Experimental cases for blending fuel combustion*

Understanding the denitrification mechanisms of coal-fired decoupling combustion grate boiler, this study further aims to investigate decoupling combustion characteristics of blending fuels such as Coal b + Straw and Coal c + Residue. Considering the high volatile content of straw pellets, a stream of burnout air was introduced into the hearth through an inlet on the partition wall (see Fig. 2) by an air fan (the FGR fan) in order to suppress possible severe fluctuation of outlet CO concentration. Moreover, as indicated in Table 3, the volume percent of burnout air increases up to 20% to 30% with increasing the blending mass fraction of straw pellets to 70%, corresponding to the decrease of primary air volume percent down to 50% to 60% at the constant pre-burning air volume percent of about 20%. Similar to the combustion of coal fuel, the total excess air coefficient of 1.3 and the uniform primary air distribution mode were still adopted in co-firing coal briquettes and straw pellets. However, because of the high water content of 50.0%, the blending mass fraction of Chinese medicine residue was controlled to be lower than 50% and the total excess air coefficient was increased to about 1.8 in order to ensure the stable operation and power supply of the test facility, while the uniform primary air distribution mode was still set in co-firing coal briquettes and medicine residue without the introduction of burnout air.

3. Results and Discussion

3.1. *Decoupling combustion characteristics of coal briquettes*

3.1.1. *Optimization of fuel bed depth and air distribution mode*

Fig. 3 shows the temperature and species concentration profiles in the hearth under different operation cases. On the whole, the temperature in the hearth is generally lower than 1000 °C at the points of T1–T4, but high up to about 1200 °C at the points of T5 and T6 in all the cases. The O_2 concentration remarkably decreases from point a to b in all the cases because of the rapid ignition of fresh coal particles in the top layer of fuel bed, and then levels off at the points of c and d in Cases II–IV or slightly increases again at the two points in Cases I and V. As expected, a low temperature oxygen-deficient pyrolysis and combustion zone forms in the front section of hearth and is followed by a high temperature air burnout zone in the rear section of hearth. The oxidizing atmosphere in the rear high temperature burnout zone can be enhanced by adopting either the small fuel bed depth in Case I or the rear-enhanced air distribution mode in Case V. However, this enhanced oxidizing atmosphere leads to a clear increase of NO_x concentration at the points of c and d, but has little positive effect on the decrease of CO concentration there because of the high temperature at the two points.

To be specific, increasing the fuel bed depth from 120 to 180 mm under the uniform air distribution mode as Cases I–III denote, both the O_2 and NO_x concentrations clearly decrease at the points of b–d, but the CO concentration obviously increases at the points of a and b. These are because the increase of fuel bed depth increases heterogeneous combustion intensity and O_2 consumption in the fuel bed, thereby generating a large amount of CO in a short time, especially under the low temperature oxygen-deficient atmosphere in the front section of hearth. Under this situation, both the conversion of volatile N to NO_x in the front section of hearth and the oxidization of char N to NO_x in the rear section of grate are suppressed simultaneously [14,15,29]. At the fixed fuel bed depth of 180 mm, adopting the front-lean air distribution mode in Case IV enables the rapid ignition of more fuel particles, so the O_2 concentration maintains nearly invariant but the CO concentration increases a lot at the points of a–c in comparison with Case III. Similar to the increase of fuel bed depth, this is because CO is not easy to be ignited and burned off at the low temperature of 700–1000 °C in the front section of hearth. However, most of the CO can still be combusted at the rear high-temperature zone of hearth, while the release of a large amount of fuel N in advance leads to the increase of NO_x concentration at all the points [30]. On the contrary, adopting the rear-enhanced air distribution mode in Case V, the fuel combustion was delayed and extended to the rear grate in comparison with Case III, thus resulting in local excess of O_2 at the points of c and d. Comparing Case V with Case III, lower NO_x and CO concentrations at the points of a and b are mainly because the generation of NO_x and CO is reduced under the condition of low pyrolysis and combustion

Table 2
Three typical air distribution modes for coal combustion.

Air distribution mode	Pre-burning air/% (vol)	Primary air/% (vol)				
		i	ii	iii	iv	v
Uniform (I–III)	18–22	19–22	14–16	14–16	13–15	14–16
Front-lean (IV)		30–35	15–20	13–15	5–8	7–10
Rear-enhanced (V)		16–18	11–13	9–11	18–20	18–20

Table 3
Air distribution mode for co-firing straw pellets.

Blending fraction/% (mass)	Air distribution mode/% (vol)		
	Pre-burning air	Primary air	Burnout air
0	18–22	~80	0
30		70–80	3–7
50		60–70	10–20
70		50–60	20–30
100		40–50	30–40

intensity, while higher NO_x and nearly constant CO concentrations at the points of c and d are mainly caused by the enhanced high temperature oxidizing atmosphere, which is in favor of the generation of NO_x and the burnout of CO.

The relative contents of NO_x and O_2 in flue gas can be expected to remain invariant under the different operation cases beyond the point d because the coke combustion intensity is very weak and the release of fuel NO_x nearly stops in the rear fuel bed. However, the CO concentration beyond the point d may be reduced further at the flue gas temperature higher than about 1200 °C because the mixing intensity of flue gas is significantly strengthened by the comprehensive action of partition wall and rear arch. As shown in Fig. 4, the outlet NO_x and O_2 concentrations gradually decrease with increasing the fuel bed depth from 120 to 180 mm, which can be as low as 103 $mg \cdot m^{-3}$ and 8.61% in Case III, respectively. Compared to the NO_x emissions of about 325 $mg \cdot m^{-3}$ in traditional grate boilers burning bituminous coal [8], the reduction of NO_x emissions is high up to 68.3% in the novel decoupling combustion grate boiler, which is much higher than the NO_x reduction of 25% under the condition of implementing the decoupling combustion technology partially [19]. As discussed before, this is because the large fuel bed depth calls for the consumption of much more O_2, which can also suppress the conversion of fuel N to NO_x and facilitate the reduction of NO_x by pyrolysis gas and char layer. The outlet CO concentration of 46 $mg \cdot m^{-3}$ in Case III is much lower than that at the point d and is also the lowest in Cases I–III. It can be mainly attributed to the increase of residence time of solid fuel as well as the aforementioned influences. Compared to Case III, the front-lean air distribution mode in Case IV favors the occurrence of fuel pyrolysis and combustion processes in advance, which results in further reduction of the outlet CO and O_2 concentrations (43 $mg \cdot m^{-3}$ and 7.06%). The release of fuel N in advance and the centralized formation of NO_x in the front section of hearth in Case IV cause the higher outlet NO_x concentration (120 $mg \cdot m^{-3}$) than in Case III. Under the rear-enhanced air distribution mode in Case V, the outlet O_2 concentration increases correspondingly. The enhanced oxidizing atmosphere in the rear hearth promotes the conversion of fuel N to NO_x, leading to the secondary high outlet NO_x concentration of 133 $mg \cdot m^{-3}$ in all the cases. The strengthened mixing intensity of high temperature flue gas together with the increased O_2 concentration in Case V favors the burnout of CO, giving rise to the lowest outlet CO concentration of 27 $mg \cdot m^{-3}$ in all the cases. This also demonstrates the advantages of decoupling combustion grate boiler in reducing CO emission and improving thermal efficiency.

It is worth noting that the slag carbon content in Cases I–III is generally lower than 10.00%, even down to 8.40% in Case III, which can be similarly attributed to the large residence time of solid fuel at the large fuel bed depth as well as the high coal combustion

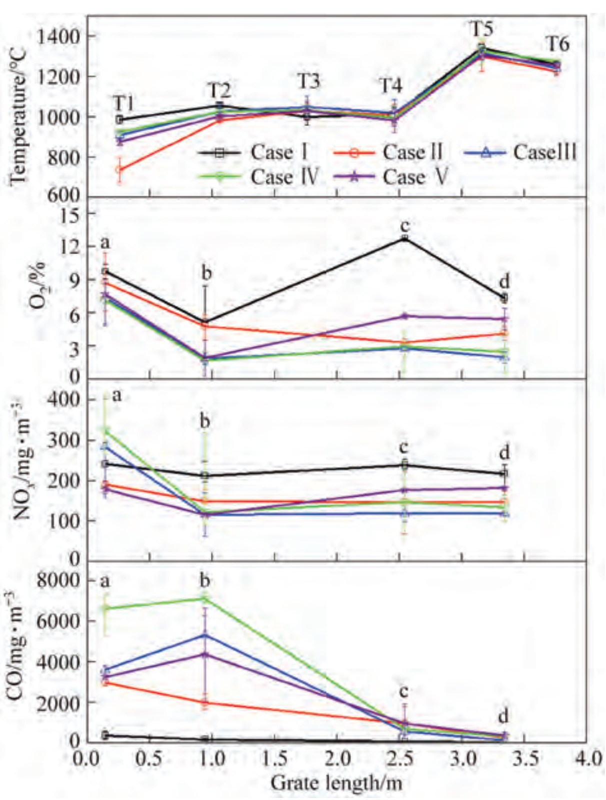

Fig. 3. Temperature and species concentration profiles under the different cases.

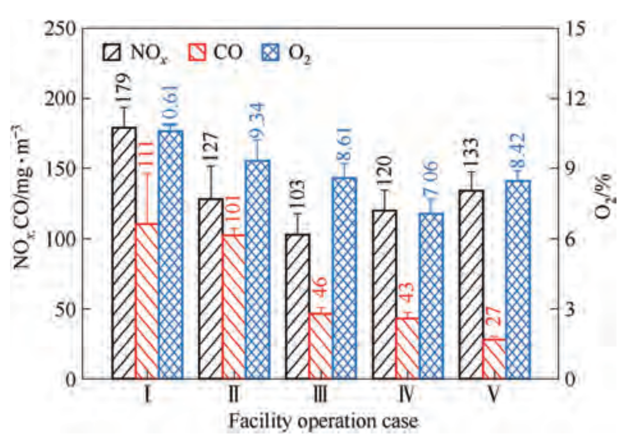

Fig. 4. Outlet species concentrations under the different cases.

efficiency under the condition of decoupling combustion. The slag carbon content for the front-lean air distribution mode of Case IV further decreases to 7.31% because the pyrolysis and combustion processes happen in advance, while the slag carbon content at the rear-enhanced air distribution mode in Case V reversely increases to 10.16% because the char combustion process is postponed significantly and cannot proceeds completely. Regardless of air distribution modes, the slag carbon content in the novel decoupling combustion grate boiler is always rather lower than the average amount of slag carbon content of about 10% to 15% in traditional coal-fired grate boiler. It is clear that Case III adopting the fuel bed depth of 180 mm and the uniform air distribution mode has the best comprehensive effectiveness in reducing pollutant emission and improving combustion efficiency. Under these optimal conditions, the thermal efficiency of the pilot-scale test facility calculated from dividing the total caloric content of fuel by the total heat of circulating water per unit time is higher than 80.0% in the case of burning bituminous coal briquettes.

3.1.2. Combination of decoupling combustion and flue gas recirculation

Using Case III as a benchmark with the zero FGR ratio, the combination of decoupling combustion with two FGR modes was investigated comparatively. As shown in Fig. 2, by using the flue gas recirculating fun, in the hearth FGR a proportion of flue gas with the temperature of about 473 K and the O_2 concentration of about 8.6% was recirculated into the middle rear hearth, while in the windbox FGR a small amount of flue gas was first mixed with primary air and then supplied into the five windboxes under the uniform air distribution mode.

The hearth FGR lowers the hearth temperature while increases the O_2 concentration and the turbulence intensity in the combustion zone, so affecting the conversion of volatile N to NO_x and the burnout of gas combustibles [31], especially in the decoupling combustion boiler. The former impedes the burnout of CO and the conversion of volatile N to NO_x, but the latter contributes to the above two processes. It is clear that the implementation of hearth FGR has two opposite impacts on the CO and NO_x concentrations, so an optimal hearth FRG ratio may exist for reducing NO_x and CO emissions simultaneously in the decoupling combustion grate boiler [32]. As shown in Fig. 5, the outlet NO_x and CO concentrations decrease to be as low as 86 and 35 $mg\cdot m^{-3}$, respectively, when the hearth FGR ratio increases from zero to 14%, further giving rise to 16.5% and 23.9% reduction of NO_x and CO emissions in comparison with the benchmark case, respectively. However, further increasing the hearth FGR ratio to 24% causes a slight increase of outlet NO_x concentration due to the NO_x accumulation effect associated with the large hearth FGR ratio [33,34], though the outlet CO concentration further decreases to 30 $mg\cdot m^{-3}$. The resulted decrease of hearth temperature from the hearth FGR also exerts a negative effect on the combustion of fuel bed, so the slag carbon content at the hearth ratio of 14% is about 9.10%, which is higher than 8.40% in the benchmark case.

Different from the hearth FGR, the windbox FGR always decreases the O_2 content in the primary air, which may decrease the heterogeneous combustion intensity in the fuel bed, especially under the bottom-to-top combustion mode. As a result, the temperatures in both the fuel bed and the boiler hearth show obvious decreases under the condition of windbox FGR. The combined action of the decreased combustion temperature and primary air O_2 concentration clearly suppresses the formation of NO_x from char N but contributes much to the incomplete combustion of coal char [10,35]. Nevertheless, a further increase of the windbox FGR may lead to the excess O_2 concentration in the hearth because of the decreased O_2 consumption in the fuel bed, and further benefit for burning CO in the hearth. Under this situation, the NO_x concentration may increase because the generation of NO_x from volatile N is promoted in the hearth [36]. Accordingly, as shown in Fig. 6, the windbox FGR ratio of 11% achieves the best effectiveness in terms of the reduction of NO_x and CO emissions when the windbox FGR ratio ranges from 5% to 16%. At the optimal windbox FGR ratio, the outlet NO_x and CO concentrations are as low as 80 and 36 $mg\cdot m^{-3}$, corresponding to the 22.3% and 21.7% reduction of NO_x and CO emissions, respectively, in comparison with the benchmark case. This phenomenon also indicates a higher denitrification efficiency of windbox FGR than that of hearth FGR. Similarly, the windbox FGR has a much more significant effect on the combustion temperature of fuel bed than the hearth FGR. Compared to the slag carbon content of 8.40% in the benchmark case, the slag carbon contents at the windbox FGR ratios of 5%, 11% and 16% are approximately 10.64%, 10.95% and 11.11%, respectively. Therefore, much attention should be paid to the influences of the windbox FGR on the incomplete combustion of gas and solid combustibles in the decoupling combustion coal-fired grate boiler.

It is clear that the hearth FGR tends to affect much the combustion of coal volatiles and the conversion of volatile N, while the windbox FGR exerts more impacts on the combustion of coal char and the conversion of char N. By adopting these two recirculation methods in the decoupling combustion grate boiler simultaneously, the pollutant emission can be expected to decrease further. Various hearth and windbox FGR combinations were tested in this study, and the optimal FGR combination was determined as 10% for both

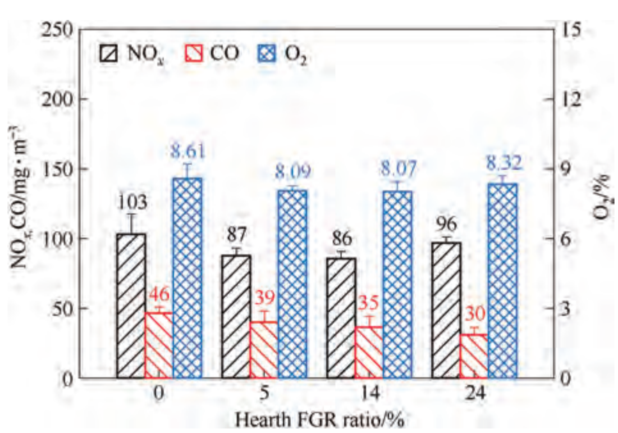

Fig. 5. Outlet species concentrations at the different hearth FGR ratios.

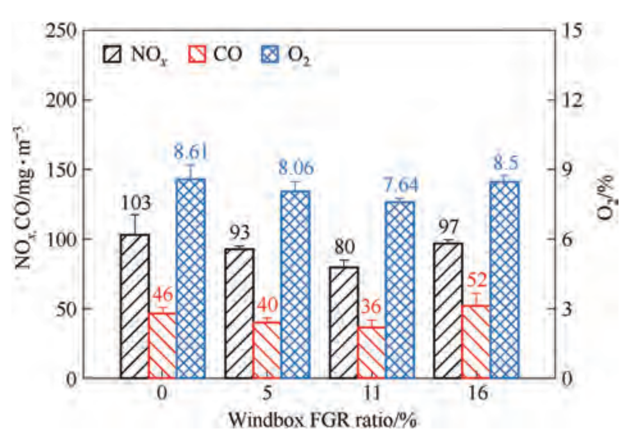

Fig. 6. Outlet species concentrations at the different windbox FGR ratios.

the hearth and windbox FGR ratios finally. As shown in Fig. 7, under the optimal FGR combination both the temperature and oxygen concentration in the entire hearth are lower than those in the benchmark case without FGR. Correspondingly, the NO_x concentrations at the four measuring points decrease remarkably in comparison with the benchmark case. Although the CO concentration at the points of a and b increases clearly due to the decreases of temperature and oxygen content in the front section of hearth, this value can also be reduced to be lower than that in the benchmark case because of the high temperature and mixing intensity in the burnout zone. In comparison with the outlet NO_x and CO concentrations of 103 and 46 mg· m^{-3} in the benchmark case respectively, the outlet NO_x concentration declines to 56 mg· m^{-3}, while the outlet CO concentration maintains nearly invariable in the optimal FGR combination. The NO_x emissions are reduced by 45.6% in comparison with the benchmark case without FGR, which is higher than the NO_x emission reduction of 10% to 30% in the traditional coal-fired grate boiler with FGR [9,10], implying the synergistic effect of combining the decoupling combustion and FGR technologies. Compared to the average NO_x emission level in traditional coal-fired grate boilers, the NO_x reduction efficiency is even high up to 82.8%, which is also superior to the NO_x reduction efficiency of 33% to 59.4% in the decoupling and reburning combinative low-NO_x coal grate boiler [18,23].

3.2. Decoupling combustion characteristics of blending fuels

3.2.1. Decoupling co-firing of coal briquettes and straw pellets

During the co-combustion of blending fuels, the NO_x emissions are dependent on fuel nitrogen content, nitrogen compound form, combustion reaction atmosphere, and even possible synergistic effect among their constituents, *etc.* Accordingly, the NO_x emissions from co-firing blending fuels cannot be simply predicted from the expected values of a linear interpolation of the corresponding emissions of their constituents [4,37]. Fig. 8 depicts the variation of outlet NO_x, CO and O_2 concentrations with the blending mass fraction of straw pellets. It is shown that both the NO_x and CO concentrations from burning Coal b separately are substantially low. As stated in subsection 2, this can be attributed to the adoption of pre-burning device and the air-staged combustion as well as the bottom-to-top ignition mode in the test facility. With the addition of straw pellets, both the NO_x and CO emission concentrations increase with increasing blending mass fraction, even the NO_x emissions of burning straw pellets separately are nearly twice those of burning Coal b separately. These can be explained by the facts that the nitrogen content of straw pellets (4.40%) is much higher than that of Coal b (1.21%) and the increased amount of burnout air was introduced in the co-combustion of coal-straw blends, which promote the oxidization of volatile-N of coal and straw at the rear of hearth. While, the increase of CO emission with increasing blending mass fraction may result from the increasing release rate of straw volatile and the thinning mixing char layer, which lead to the insufficient contact of gas combustibles and air as well as high temperature char layer. As indicated by the error bars of CO concentration, this deduction can be consolidated by gradually increasing fluctuation amplitude of outlet CO concentration with increasing blending mass fraction. It is worth noting that the outlet O_2 concentration clearly decreases with increasing blending mass fraction as the total excess air coefficient remains around constant. This is mainly because both the self-supplied oxygen from straw pellets and the oxygen consumption in the combustion of blending fuel increase relatively, since the slag carbon content of blending fuels is as low as 5.54% to 7.53%, which is lower than that of burning Coal b separately. It is clear that the variation trend of O_2 concentration is contrary to that of NO_x emissions, indicating that the formation and conversion of NO_x in the travelling-grate decoupling combustion is dominated by the reaction atmosphere and temperature profiles, rather than the total excess air coefficient alone [26].

The synergistic effect of co-firing Coal b and straw pellets may be reflected in the reduction of NO_x by the coal char layer and the straw pyrolysis gas. As shown in Fig. 8, the dashed lines denote the weighted average NO_x and CO emission values based on the experimental outlet species concentrations of the mono-combustion of either Coal b or straw pellets in the novel grate boiler, that is,

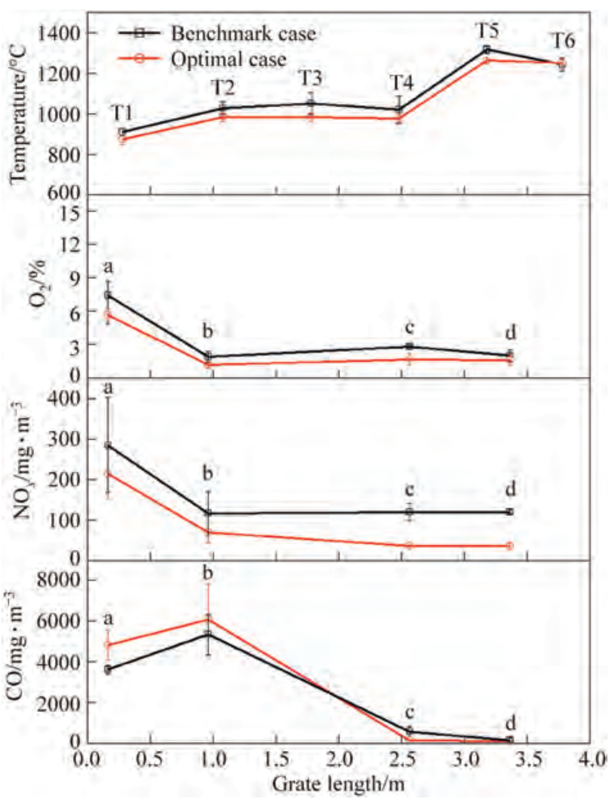

Fig. 7. Temperature and species concentration profiles in the optimal FGR case.

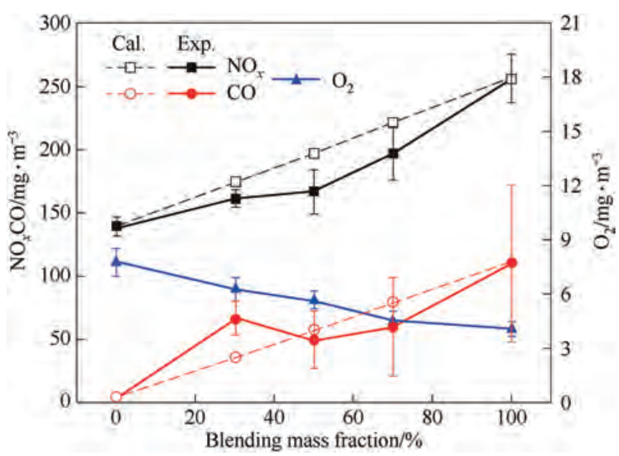

Fig. 8. Influence of blending fraction of straw pellets on outlet species concentrations.

$$C_{j,cal} = (1 - x_m) \times C_{j,coal,exp} + x_m \times C_{j,straw,exp} \quad (2)$$

where C_j is NO_x or CO emission concentration; x_m is straw blending mass fraction. Note that the calculated pollutant emission concentration represents the anticipated value estimated from the corresponding decoupling combustion emissions of blend constituents. It can be seen that the experimental NO_x emissions of blending fuels are generally lower than the calculated values, showing a possible synergistic effect between Coal b and straw pellets in suppressing NO_x emissions. Large amount of pyrolysis gases including CO and NH_3 released from straw pellets essentially provide in situ thermal denitrification sources for the decoupling combustion of blending fuels [21], especially when the oxygen consumption for fuel combustion is decreased and a local reducing atmosphere is enhanced significantly due to the high oxygen content of straw pellets [34]. However, in order to ensure a high volatile burnout ratio and a low CO emission concentration, a larger amount of burnout air has to be introduced to the rear hearth at a higher blending mass fraction, which constrains the above-mentioned synergistic effect. At the blending mass fraction of 50%, the NO_x emissions can be further mitigated by at most about 16.0% on top of the already reduced amount by decoupling combustion to reach less than about 165 $mg \cdot m^{-3}$, which is consistent with the previous experimental data of NO_x emission reduction of 10% to 27% in comparison with traditional grate combustion [3–5].

Co-firing Coal b and straw pellets also improved the combustion performance of blending fuels due to the combined action of high-reactivity straw pellets and stable coal char layer, especially in alleviating the slagging and fouling tendency [22]. Table 4 shows the ash composition data of Coal b and straw pellets, which were determined by X-ray fluorescence spectrometer (XRF, Thermo Fisher Scientific Company, USA). It is clear that Coal b ash has high contents of calcium oxide, silicon oxide and aluminum oxide, while the contents of potassium oxide and sodium oxide in the straw pellet ash are far more than in the Coal b ash, indicating that biomass pellets has a much higher slagging and fouling tendency than Coal b.

However, co-firing coal and straw may enable the formation of high-melting-point silicates to alleviate the slagging and fouling tendency [6,16]. So, X-ray diffraction analysis was performed to obtain the XRD patterns of bottom ashes, which were recorded by a PANalytical X'Pert powder X-ray diffractometer with Cu K_α radiation. The samples were scanned from $2\theta = 10^\circ - 80^\circ$ with a step size of 0.033°. As shown in Fig. 9, with the increase of blending mass fraction, the peak patterns of blending fuels start differing much from that of straw pellets, implying the variation of mineral composition of bottom ashes. Bredigite ($Ca_7MgSi_4O_{16}$) and some mineral compounds with high ash melting temperature such as calcium silicate (Ca_2SiO_4), dicalcium aluminate ($Ca_2Al_2O_5$) and spinel ($MgAl_2O_4$) are exclusively present in the bottom ashes from coal briquettes and blending fuels, while some mineral compounds with low ash melting temperature such as calcium aluminosilicate ($CaAl_2Si_2O_8$) and potassium feldspar ($KAlSi_3O_8$) only exist in the bottom ash from straw pellets. As the blending mass fraction increases from zero to 100%, the peak intensity of melilite ($Ca_2Al_2SiO_7$) with high ash melting temperature decreases gradually, and the peak even disappears when the blending mass fraction is greater than 70%. On the contrary, the peak of akermanite ($Ca_2MgSi_2O_7$) with low ash melting temperature occurs until the blending mass fraction is up to 50%, and the peak intensity increases gradually with the increase of blending mass fraction from 50% to 100%. These results indicate that the decoupling co-combustion of coal *b* and straw pellets does alleviate the slagging tendency of blending fuels in comparison with burning straw pellets separately.

Table 4
Ash composition analysis of Coal b and straw pellets.

Oxide	Ash composition (ash basis normalized to 100%)/% (mass)	
	Coal b	Straw
CaO	22.47	31.37
SiO_2	39.61	23.38
K_2O	1.18	3.55
MgO	1.46	9.62
SO_3	4.99	5.99
Al_2O_3	23.84	6.72
Na_2O	0.54	6.59
Fe_2O_3	3.27	3.39
P_2O_5	0.22	1.00
TiO_2	2.35	8.28
MnO	0.07	0.11

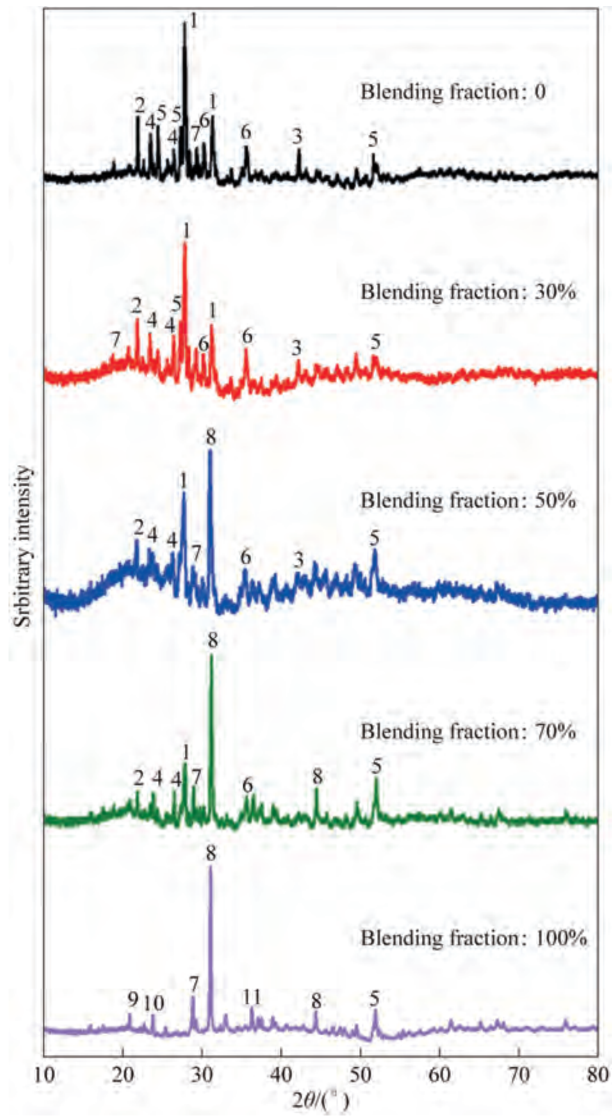

Fig. 9. XRD patterns of bottom ashes from co-firing coal briquettes and straw pellets. 1. Bredigite ($Ca_7MgSi_4O_{16}$), 2. Calcium silicate (Ca_2SiO_4), 3. Melilite ($Ca_2Al_2SiO_7$), 4. Dicalcium aluminate $Ca_2Al_2O_5$), 5. Grossite ($CaAl_4O_7$), 6. Spinel ($MgAl_2O_4$), 7. Calcio-langbeinite ($K_2Ca_2(SO_4)_3$), 8. Akermanite ($Ca_2MgSi_2O_7$), 9. Calcium aluminosilicate ($CaAl_2Si_2O_8$), 10. Potassium feldspar ($KAlSi_3O_8$), 11. Magnesium silicate (Mg_2SiO_4).

3.2.2. Decoupling co-firing of coal briquettes and medicine residue

As indicated in Table 1, the constituent properties of Chinese medicine residue on the air dried basis are very similar to those of straw pellets, but the volatile and fixed carbon contents of Coal c as well as its net calorific value are slightly lower than those of Coal b, respectively. Therefore, the probable differences of co-firing wet medicine residue and Coal c from burning straw-Coal b blends mainly result from the effects of the water content of high up to 50% in the medicine residue, because the latent heat of vaporization of a large amount of water significantly influences the hearth temperature and further the involved gasification reactions with water steam. As shown in Fig. 10, both the outlet CO and O_2 concentrations firstly decrease and then increase with increasing blending mass fraction of medicine residue, which differ much from the emission characteristics of co-firing Coal b and straw pellets. At the low blending mass fraction of 10%, the addition of medicine residue, similar to the introduction of straw pellets, promotes the combustion of blending fuels because a small amount of water carried by medicine residue has little effect on the pyrolysis process in the pre-burning device and the combustion process in the hearth, giving rise to the slight decreases of CO and O_2 concentrations. As the blending mass fraction increases up to about 20% to 30%, the effects of the char steam gasification reaction and the water-gas shift gasification reaction on the outlet species concentrations become increasingly pronounced at the reasonable hearth temperature [38], leading to the increase of CO concentration. Further increasing the blending mass fraction beyond 30% to 40%, the vaporization of a large amount of water leads to a clear decrease of temperature in both the pre-burning device and the boiler hearth, and further to the delayed release of residue and coal volatiles. Under this situation, the incomplete combustion of combustibles becomes dominant, resulting in the significantly increased CO concentration and corresponding fluctuation amplitude as well as the slightly increased O_2 concentration though the total excess air coefficient is high up to be about 1.8. When the blending mass fraction of high-water-content medicine residue is higher than about 50%, the wet blending fuel is uneasily to ignite in the pre-burning device and the test facility runs abnormally because of a marked drop and strong fluctuation of temperature in both the pre-burning device and the hearth.

Compared to burning Coal a or Coal b separately, the NO_x emissions from burning Coal *c* are reduced to a rather low level owing to the lower hearth temperature and the lower volatile and nitrogen contents of Coal c. In addition, this phenomenon may also be related to the higher CO emission in the case since there is a mutually restrictive relationship between the NO_x and CO emissions due to the reducibility of CO to NO_x [17]. However, the outlet NO_x concentration does not increase gradually with increasing the blending mass fraction of medicine residue as we observed in the co-combustion of Coal b and straw pellets, but firstly increases and then decreases to the level equivalent to that of burning Coal c separately at the blending mass fraction of 40%, and subsequently rises slightly again. This can be explained by the fact that the nitrogen content of medicine residue (1.14%) is nearly equivalent to that of Coal c (0.80%). Moreover, the reducing atmosphere in the hearth is enhanced by the generation of CO and H_2 from the gasification reactions at the blending mass fraction of about 30% to 40% in addition to the reductive actions of high temperature char layer and medicine residue volatile [38].

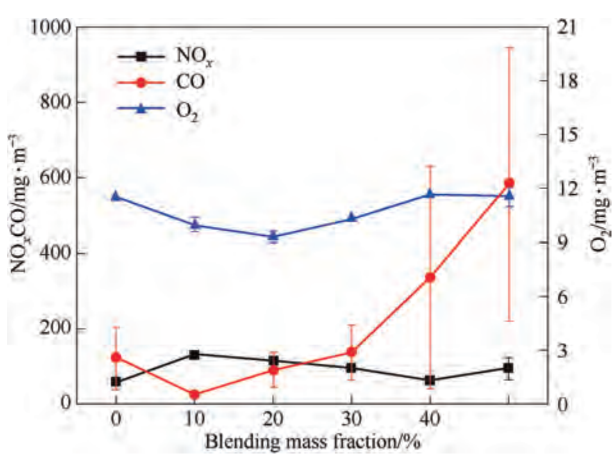

Fig. 10. Influence of blending fraction of medicine residue on outlet species concentrations.

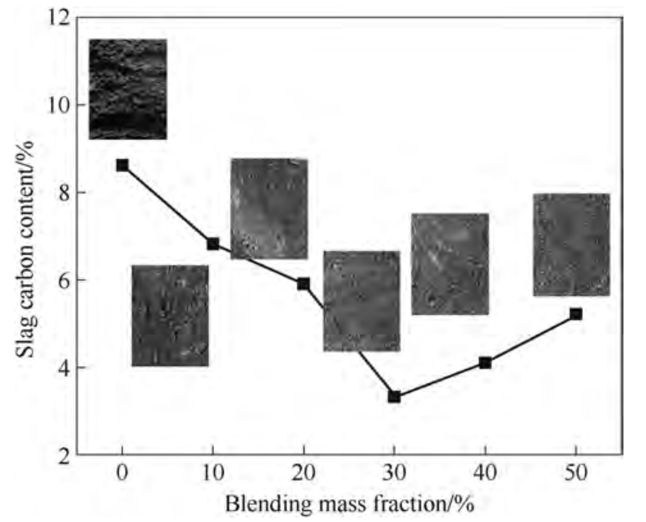

Fig. 11. Slag carbon content and bottom ash morphology of co-firing Coal *c* and medicine residue.

Fig. 11 shows the slag carbon content and bottom ash morphology of co-firing Coal c and medicine residue. As expected, the slag carbon content decreases clearly as the blending mass fraction of medicine residue increases from zero to 30% because of the mutual promotion of Coal *c* and medicine residue in combustion performance. This phenomenon also indicates that the introduction of pre-burning device significantly decreases the impact of water carried by medicine residue on the combustion behavior in the hearth. However, as discussed before, this impact cannot be ignored when the blending mass fraction of medicine residue is greater than about 30%, beyond which the slag carbon content increases gradually with increasing the blending mass fraction. These results imply that the remarkable increase of outlet CO concentration with increasing blending mass fraction results from both the heterogeneous incomplete combustion of carbon and the homogeneous incomplete combustion of CO, but the latter dominates in this case since the slag carbon content is still lower than around 5.0% at the blending mass fraction of 50%. Another point worth mentioning is that the slagging phenomenon was not observed in the bottom ashes from burning the coal-residue mixture with different blending mass fractions.

4. Conclusions

Focusing on the reduction of NO_x and CO emissions as well as slag carbon content in industrial grate boilers, the decoupling combustion characteristics of bituminous coal briquettes and their mixture with straw pellets or wet Chinese medicine residue in the pilot-scale test facility were investigated experimentally in order to demonstrate the advantages of the novel travelling grate boiler. It is the first time to integrate the decoupling combustion and flue gas recirculation or co-firing technologies in the industrial grate boiler by introducing the pre-burning device instead of the fuel feeder and simplifying the front and rear arches in the traditional travelling grate boiler.

Burning bituminous coal briquettes separately, the travelling grate decoupling combustion technology can facilitate the original NO_x emission reduction of 68.3% in comparison with the average value in traditional coal-fired grate boilers, which can be further improved to 82.8% by integrating the flue gas recirculation technology, thus meeting the ultra-low emission standard for industrial coal-fired grate boilers directly. Correspondingly, the slag carbon content is decreased to be lower than about 10.0%, indicating the high combustion efficiency in the novel grate boiler. Co-firing coal briquettes with straw pellets in the novel grate boiler, the NO_x emissions are lower than the anticipated one and can be further mitigated by at most 16.0% on top of the already reduced amount by decoupling combustion. The blending mass fraction of Chinese medicine residue can be high up to 30% on the premise of low NO_x and CO emissions in the novel grate boiler, showing its higher fuel adaptability to co-firing wet biomass wastes. All co-firing experiments also demonstrated the synergistic effects of co-firing coal-biomass blends in mitigating slagging tendency and slag carbon content in the novel grate boiler.

Though the feasibility and superiority of the newly-developed travelling grate decoupling combustion technology were experimentally validated in the pilot-scale test facility, its application in large-scale industrial travelling grate boilers still needs to be implemented in future work. Considering the energy resource characteristics and environmental protection policies in China, the decoupling combustion and flue gas recirculation combinative technology can be economically used to upgrade the existing industrial coal-fired grate boilers by replacing their fuel feeders with the pre-burning devices, so as to provide a novel measure for the ultra-low NO_x emission transformation of industrial coal-fired grate boilers, while the decoupling and co-firing combinative technology can be conveniently utilized to promote the clean and highly efficient consumption of biomass wastes with high water content or difficulty to burn.

CRediT Authorship Contribution Statement

Xinhua Liu: Writing – review & editing, Supervision, Funding acquisition, Writing – original draft, Methodology, Conceptualization. Bin Liang: Validation, Methodology, Investigation. Jian Han: Methodology, Validation, Investigation. Shanwei Hu: Supervision, Conceptualization, Writing – original draft, Investigation.

Declaration of Competing Interest

The authors declare that they have no known competing financial interests or personal relationships that could have appeared to influence the work reported in this paper.

Acknowledgements

We would like to thank senior engineers Xue Bai and Jiangping Hao for their help in preparing the manuscript. This research was supported by the Strategic Priority Research Programs of Chinese Academy of Sciences (XDA29020401) and the Fund of State Key Laboratory of Mesoscience and Engineering (Meso-23-A02).

References

[1] X. Liu, X.Y. Zhang, R.E. Zhang, X.D. Yang, M. Shan, Y.Q. Liu, Report on Chinese Urban Scattered Coal Management, Energy Foundation, Tsinghua University Research Center of Building Energy Efficiency, Beijing, 2022.

[2] M.A. Koondhar, Z. Tan, G.M. Alam, Z.A. Khan, L. Wang, R. Kong, Bioenergy consumption, carbon emissions, and agricultural bioeconomic growth: a systematic approach to carbon neutrality in China, *J. Environ. Manag.* 296 (2021) 113242.

[3] E. Rokni, X.H. Ren, A. Panahi, Y.A. Levendis, Emissions of SO_2, NO_x, CO_2, and HCl from co-firing of coals with raw and torrefied biomass fuels, *Fuel* 211 (2018) 363–374.

[4] X.J. Liao, S.H. Zhang, X.C. Wang, J.N. Shao, X. Zhang, X.H. Wang, H.P. Yang, H.P. Chen, Co-combustion of wheat straw and camphor wood with coal slime: Thermal behaviour, kinetics, and gaseous pollutant emission characteristics, *Energy* 234 (2021) 121292.

[5] X.D. Yang, Z.Y. Luo, X.R. Liu, C.J. Yu, Y.A. Li, Y.C. Ma, Experimental and numerical investigation of the combustion characteristics and NO emission behaviour during the co-combustion of biomass and coal, *Fuel* 287 (2021) 119383.

[6] T. Madhiyanon, P. Sathitruangsak, S. Sungworagarn, T. Udomman, Investigation of rice-straw-ash fouling/slagging and countermeasures using supplementary additives and co-firing with Si–Al-rich coal in a pilot-scale grate-fired combustor, *J. Energy Inst.* 93 (5) (2020) 1848–1867.

[7] S.G. Sahu, N. Chakraborty, P. Sarkar, Coal–biomass co-combustion: an overview, *Renew. Sustain. Energy Rev.* 39 (2014) 575–586.

[8] J.P. Hao, S.Q. Gao, G.F. Sun, J.D. He, Status of coal-fired industrial boilers and development of decoupling combustion technique, *Ind. Boil. (4) (2014) 7–11.*

[9] G. Liuzzo, N. Verdone, M. Bravi, The benefits of flue gas recirculation in waste incineration, *Waste Manag.* 27 (1) (2007) 106–116.

[10] L. Xu, G.B. Zhao, J.M. Gao, Q. Du, J.Y. Luan, L.F. Zhao, Y. Zhang, S.H. Wu, Effect of flue gas recirculation on nitric oxide (NO) emissions during the coal grate-fired process, *Toxicol. Environ. Chem.* 99 (5–6) (2017) 783–794.

[11] Y. Lei, Y. Liu, Y.Q. Niu, S.E. Hui, Research on SNCR/flue gas recycling synergistic denitration technology, *Clean Coal Technol.* 25 (3) (2019) 110–115 (in Chinese).

[12] X.C. Yang, Y.F. Liao, Y.Q. Wang, X.F. Chen, X.Q. Ma, Research of coupling technologies on NO_x reduction in a municipal solid waste incinerator, *Fuel* 314 (2022) 122769.

[13] J.H. Li, Y.R. Bai, W.L. Song, NO_x-suppressed smokeless coal combustion technique, Proceedings of international symposium on clean coal technology, *Chin. J. Process Eng.* 1 (2001) 95–98 (in Chinese).

[14] J.D. He, W.L. Song, S.Q. Gao, L. Dong, M. Barz, J.H. Li, W.G. Lin, Experimental study of the reduction mechanisms of NO emission in decoupling combustion of coal, *Fuel Process. Technol.* 87 (9) (2006) 803–810.

[15] H.L. Li, J. Han, N. Zhang, X.H. Liu, J.D. He, W. Du, Effects of high-temperature char layer and pyrolysis gas on NO_x reduction in a typical decoupling combustion coal-fired stove, *J. Therm. Sci.* 28 (1) (2019) 40–50.

[16] B. Liang, H.L. Bai, D.R. Bai, X.H. Liu, Emissions of non-methane hydrocarbons and typical volatile organic compounds from various grate-firing coal furnaces, *Atmos. Pollut. Res.* 13 (4) (2022) 101380.

[17] J. Han, X.H. Liu, S.W. Hu, N. Zhang, J.J. Wang, B. Liang, Optimization of decoupling combustion characteristics of coal briquettes and biomass pellets in household stoves, *Chin. J. Chem. Eng.* 59 (2023) 182–192.

[18] L.G. Cai, X. Shang, S.Q. Gao, Y. Wang, L. Dong, G.W. Xu, Low-NO_x coal combustion *via* combining decoupling combustion and gas reburning, *Fuel* 112 (2013) 695–703.

[19] H.M. Wang, L.P. Song, X.H. Yang, Z.P. Liu, X.H. Liu, N. Zhang, J.P. Hao, T. Lan, Application of pre-burning low-NOx combustion technology in industrial coal-fired grate boilers, *Coal Proc. Comp. Utilization* (6) (2019) 83–87 (in Chinese).

[20] L. Dong, S.Q. Gao, W.L. Song, J.H. Li, G.W. Xu, NO reduction in decoupling combustion of biomass and biomass–coal blend, *Energy Fuel.* 23 (1) (2009) 224–228.

[21] S. Munir, W. Nimmo, B.M. Gibbs, The effect of air staged, co-combustion of pulverised coal and biomass blends on NO_x emissions and combustion efficiency, *Fuel* 90 (1) (2011) 126–135.

[22] B. Liang, X.H. Liu, Decoupling combustion characteristics of biomass pellets and their mixture with bituminous briquettes, *Environ. Technol. Innov.* 32 (2023) 103275.

[23] J. Wang, H.H. Lou, F.L. Yang, F.Q. Cheng, Numerical simulation of a decoupling and re-burning combinative Low-NO_x coal grate boiler, *J. Clean. Prod.* 188 (2018) 977–988.

[24] L.D. Smoot, S.C. Hill, H. Xu, NO_x control through reburning, *Prog. Energy Combust. Sci.* 24 (1998) 385–408.

[25] P.H. Qiu, S.H. Wu, S.Z. Sun, H. Liu, L.B. Yang, G.Z. Wang, Industrial test on coal re-burning at a 600 MW utility boiler and NO_x reduction, *Kor. J. Chem. Eng.* 24 (4) (2007) 683–687.

[26] X.H. Liu, Z.N. Han, J. Han, B. Liang, N. Zhang, S.W. Hu, D.R. Bai, G.W. Xu, Principle and technology of low-NO_x decoupling combustion based on restructuring reactions, *CIE J.* 73 (8) (2022) 3355–3368 (in Chinese).

[27] S. Onenc, S. Retschitzegger, N. Evic, N. Kienzl, J. Yanik, Characteristics and synergistic effects of co-combustion of carbonaceous wastes with coal, *Waste Manag.* 71 (2018) 192–199.

[28] B.Y. Yang, J.M. Gao, L. Xu, J. Xu, Q. Du, F.G. Zhang, L. Chen, G.B. Zhao, S.H. Wu, Effect of temperature and reaction atmosphere on nitric oxide emission

during a char grate-fired process in local flue gas recirculation, *Can. J. Chem. Eng.* 99 (2021) S97−S113.

[29] H.L. Du, M. Zhang, Y.L. Zhang, Y.H. Luo, Characteristics of NO reduction by char layer in fixed-bed coal combustion, *Energy Sources Part A Recovery Util, Environ. Eff.* 39 (10) (2017) 963−970.

[30] J.J. Ji, Y.H. Luo, P.Y. Lin, Effects of air distribution and refractory arch design on efficiency of coal fired travelling grate boilers, *J. Energy Inst.* 80 (4) (2007) 214−222.

[31] B. Rajh, C.G. Yin, N. Samec, M. Hriberšek, M. Zadravec, Advanced modelling and testing of a 13MWth waste wood-fired grate boiler with recycled flue gas, *Energy Convers. Manag.* 125 (2016) 230−241.

[32] J. Liu, X.Y. Luo, S. Yao, Q.G. Li, W.S. Wang, Influence of flue gas recirculation on the performance of incinerator-waste heat boiler and NO_x emission in a 500 t/d waste-to-energy plant, *Waste Manag.* 105 (2020) 450−456.

[33] X.W. Guo, J. Zhang, Z.X. Zhang, Z.S. Yuan, J.J. Fan, B.M. Chen, Test study of new flue gas re-circulation techniques working on NO_x removal in chain-stoked boiler, *Energy Eng. J. Assoc. Energy Eng.* 4 (2017) 48−52. (in Chinese)

[34] C. Sun, J. Zhang, Z.X. Zhang, X.W. Guo, Impacts of recycled-flue-gas rate on oxygen level and NO_x emission, *J. Eng. Therm. Energy Power* 34 (5) (2019) 91−96. (in Chinese)

[35] J.Y. Luan, J.M. Gao, X.M. Wu, D.W. Shao, Study of the industrial experiment of the influence of the flue gases recycled into sections in a chain grate boiler on the operation and NO_x emissions characteristics of the boiler, *J. Eng. Therm. Energy Power* 32 (10) (2017) 90−94. (in Chinese)

[36] S. Du, J.J. Fan, Z.X. Zhang, X.W. Guo, L.Y. Zhang, Multilayer flue gas recirculation techniques on NO_x removal in chain-stoked boiler, *Clean Coal Technol* 24 (3) (2018) 103−107. (in Chinese)

[37] J. Yanik, G. Duman, O. Karlström, A. Brink, NO and SO_2 emissions from combustion of raw and torrefied biomasses and their blends with lignite, *J. Environ. Manag.* 227 (2018) 155−161.

[38] Z.N. Han, X. Zeng, C.B. Yao, Y. Wang, G.W. Xu, Comparison of direct combustion in a circulating fluidized bed system and decoupling combustion in a dual fluidized bed system for distilled spirit lees, *Energy Fuel.* 30 (3) (2016) 1693−1700.